BMBAD BJESR Mühendislik Bilimleri ve Araştırmaları Dergisi
Journal of Engineering Sciences and Researches

Optimizing Distribution Network Reconfiguration for Power Loss and Fault Current Management

Güç Kaybı ve Arıza Akımı Yönetimi için Dağıtım Şebekesi Yeniden Yapılandırmasının Optimize Edilmesi

[1]Fırat AKIN , [2]Murat ÇIKAN , [3]Oktay ARIKAN , [4]Bedri KEKEZOĞLU

[1,3,4]Yıldız Teknik Üniversitesi, Elektrik-Elektronik Fakültesi, İstanbul, Türkiye

[2]Çukurova Üniversitesi, Adana Organize Sanayi Bölgesi Teknik Bilimler Meslek Yüksekokulu, Adana, Türkiye

[1]fakin@yildiz.edu.tr, [2]mcikan@cu.edu.tr
[3]oarikan@yildiz.edu.tr, [4]bkekez@yildiz.edu.tr

Araştırma Makalesi/Research Article

ARTICLE INFO

Article history

Received : 16 June 2024
Accepted : 7 August 2024

Keywords:

Reconfiguration, Power Losses, Walrus Optimizer, 3-phase Fault Current, Meta-heuristic

ABSTRACT

This study investigates the use of network reconfiguration as a cost-effective method to optimize power system performance through the minimization of fault currents and power losses. In single-objective optimizations, the study targets the reduction of the average fault current of the buses and the power losses individually. Additionally, a multi-objective optimization study is conducted to address both parameters simultaneously. Optimization scenarios are applied on 33-bus test system through Walrus Optimizer. The results demonstrate that reconfiguration can significantly reduce power losses and fault currents, compared to the base configuration of the test system, which had a power loss of 202.60 kW and an average fault current of 2.60 p.u. Single-objective optimizations reduced power losses to 139.551 kW and minimized average fault current to 2.130 p.u. Furthermore, the multi-objective optimization provided a range of Pareto optimal solutions, examining both criteria and highlighting the flexibility of reconfiguration in adapting to power system needs.

MAKALE BİLGİSİ

Makale Tarihleri

Gönderim : 16 Haziran 2024
Kabul : 7 Ağustos 2024

Anahtar Kelimeler:

Rekonfigürasyon, Güç Kayıpları, Walrus Optimizer, Üç Faz Arıza Akımı, Meta-sezgisel

ÖZET

Bu çalışma, ekonomik bir yöntem olan şebeke yeniden yapılandırmasını, arıza akımları ve güç kayıplarının en aza indirilmesi yoluyla güç sistemi performansını optimize etmek için incelemektedir. Gerçekleştirilen tek amaçlı optimizasyon çalışmaları ile hatlardaki ortalama arıza akımının ve güç kayıplarının azaltılması ayrı ayrı hedeflemektedir. Ayrıca, her iki parametreyi aynı anda ele alan bir çok amaçlı optimizasyon çalışması da yürütülmüştür. Optimizasyon senaryoları, 33 baralı test sisteminde Walrus Optimizer algoritması kullanılarak uygulanmıştır. Sonuçlar, yeniden yapılandırmanın, test sisteminin 202.60 kW güç kaybı ve 2.60 p.u. ortalama arıza akımına sahip baz yapılandırmasına kıyasla güç kayıplarını ve arıza akımlarını önemli ölçüde azaltabildiğini göstermektedir. Tek hedefli optimizasyon çalışmaları, güç kayıplarını 139.551 kW'a ve ortalama arıza akımını 2.130 p.u.'ya düşürmüştür. Ayrıca, çok amaçlı optimizasyon çalışması, her iki kriteri de inceleyerek Pareto optimal çözümler aralığı sunmuş ve yeniden yapılandırmanın güç sistemi ihtiyaçlarına uyum sağlama konusundaki esnekliğini vurgulamıştır.

ORCID ID: [1]0000-0003-3523-2023
[2]0000-0001-6723-5769
[3]0000-0002-3304-3766
[4]0000-0002-1202-913X

Nomenclature

Abbreviations

WO	Walrus Optimizer
FCL	Fault current limiter
PSO	Particle swarm optimization
DG	Distributed generation
DQPSO	Discrete quantum PSO
MILP	Mixed-integer linear programming
GWO	Grey wolf optimization
AFC	Average three-phase fault current of the buses

Power loss calculation variables

$P^{l}_{j,k}$	Active power loss of the line between j^{th} and k^{th} buses
P^{l}_{Total}	Total active power loss of the test system
$r_{i,k}$	Resistance of the line between j^{th} and k^{th} buses
$I_{i,k}$	Current of the line between j^{th} and k^{th} buses
V_k	Voltage of the bus k
P_k, Q_k	Active and reactive power at k^{th} bus
$SW_{(j,k)}$	Status of the line between j^{th} and k^{th} buses

Radiality

N_{OS}	Number of the opened switches
N_{CS}	Number of the closed switches
N_{Line}	Number of the lines
N_{Bus}	Number of the buses
N_{Source}	Number of the sources
$\hat{A}$	Bus incidence matrix
a_{ii}	Elements of the bus incidence matrix

Fault calculation variables

U_0	Pre-fault voltage of the bus
Z_{nn}	Self-impedance of the bus
$y_{11} .. y_{nn} .. y_{NN}$	Elements of the admittance matrix
I^{f}_{n}	Three-phase fault current of bus n
I_{AFC}	Avg. three-phase fault current of test system

WO Algorithm parameters

L_{bound}	lower boundary
U_{bound}	upper boundary
t	iteration number
T	maximum iteration limit
n	population size
d	dimension of variables
M and F	male and female walrus
r / rand(.)	random number
O	reference safety position
α	constant value (chosen 1.5)
β	the migration step control factor
$f_{n,d}$	fitness values for agents
$X^{t+1}_{i,j}$	updated position for the i^{th} walrus
$X^{t}_{i,j}$	current position for the i^{th} walrus
X^{t}_{best}	the lead walrus position
$F^{t+1}_{i,j}$	next position for the i^{th} female walrus
$F^{t}_{i,j}$	current position for the i^{th} female walrus
$J^{t+1}_{i,j}$	next position for the i^{th} immature
$J^{t}_{i,j}$	current position for the i^{th} immature
X^{t}_{m} , X^{t}_{n}	denotes positions of two randomly selected walrus from the population
$X_{n,d}$	search agents' (walrus) positions
P	distress coefficient of immature walrus
LF	random numbers based on Levy distribution

1. INTRODUCTION

The global rise in population and advancements in technology are incrementally driving up the demand for electrical energy. In response to this growing need, new power plants are being brought into operation. This development results in elevated short-circuit powers and short-circuit currents within electrical power systems. Additionally, the increased load levels on the electrical power systems leads to higher power losses, which negatively effects the efficiency and reliability of power distribution. Minimizing the power losses and fault currents is crucial for the modern power systems as they increase the operational costs and can impact the overall stability and reliability.

For the mitigation of fault currents, equipment-based solutions such as reactors [1,2], high-impedance transformers [3,4], and modern fault current limiters (FCL) [5,6] are preferred, along with operational methods such as bus splitting [7,8], and feeder reconfiguration [9,10]. Feeder reconfiguration emerges as an economical solution to limit fault currents as it does not require additional equipment. In addition, it can offer different solutions according to the requirements of power systems, as it can be useful in several issues such as enhancing power quality [11], minimizing power losses [12] and improving the voltage profile of the power systems [13]. There are numerous studies in the literature that focus on enhancing power systems by addressing power losses and fault currents through reconfiguration. A. Amin et al. conducted an optimal reconfiguration study with an enhanced Brute-Force algorithm to reduce fault currents in power systems, considering both steady-state stability and generator rotor angle stability [14]. D. Topolanek et al. have studied the reduction of fault currents on a real distribution system through reconfiguration approaches involving bus splitting and area separation methods [15]. In [16], an algorithm based on Particle Swarm Optimization (PSO) is used for the optimal reconfiguration of IEEE 83-Bus distribution system to mitigate fault currents within the suitable voltage profiles of the buses. In [17], a graph theory-based method is proposed for reconfiguration considering loadability and short circuit capacity to enhance network security and reliability. In [18], a mixed-integer linear programming (MILP) model is developed for unit commitment and transmission switching. The study focuses on short-circuit current levels to enhance renewable energy integration while ensuring system protection and reliability. systems in another paper [19], an optimal reconfiguration study was conducted using a PSO-based algorithm to mitigate fault currents in the power system in case of failure of the existing FCL equipment.

In [20], which aims to reduce power losses through feeder reconfiguration, the line topologies of IEEE-33 and IEEE-69 bus test systems, which include different distributed generation (DG) models, have been optimized using Discrete Quantum Particle Swarm Optimization (DQPSO). In [21], the power losses of IEEE test systems and a real distribution system in Brazil have been reduced through a feeder reconfiguration study conducted using MILP. During the study, new linear approaches for line losses and DG integration were introduced. In [22], a hybrid algorithm consists of Grey Wolf Optimization (GWO) and PSO is employed to address total losses through feeder reconfiguration. During the study, diverse forms of distributed generation (DG) integration were implemented before, after, and during the reconfiguration process across different scenarios. Finally, the results of the scenarios are comparatively analyzed. Kamel et al. have introduced a novel application of the Geometric Mean Optimization algorithm combined with the Power Loss Sensitivity Index to address optimal network reconfiguration and DG unit allocation in distribution networks. The study aims to maximize the Voltage Stability Index and minimize total active power loss and voltage deviation [23]. In another study, the uncertainties in power generation and consumption are taken into account during the network reconfiguration to reduce power losses in several IEEE test systems that includes distributed generation [24]. L. H. Macedo et al. have conducted various optimal reconfiguration studies on an 84-bus test system to reduce total power losses while allowing closed-loop operation [25]. To mitigate the increase in fault currents, which is the main disadvantage of closed-loop operation, the fault current on the buses was allowed to increase by a maximum of 25%.

In this study, Walrus Optimizer is employed to perform optimal feeder reconfiguration including multiple scenarios on the IEEE-33 bus test system. During the investigation, it is aimed to reduce fault currents and power losses individually through separate cases. Additionally, a multi-objective optimization study was conducted to address both criteria simultaneously. Meanwhile, bus voltages are maintained within appropriate values. The results highlight that feeder reconfiguration can effectively address different criteria such as reliability and economic considerations in power systems.

The main contributions of this study to the literature are as follows:

- In this paper, a novel application of the Walrus Optimizer algorithm for optimal feeder reconfiguration in the IEEE-33 bus test system is introduced.
- The test system investigated through single-objective and multi-objective optimization cases to minimize power losses and average three-phase fault currents under the suitable bus voltage profiles.
- The results provide new insights into the trade-offs between fault current mitigation and power loss reduction. Also, outcomes highlight the potential of feeder reconfiguration to enhance power system reliability and economic efficiency by addressing various operational criteria.

2. THEORETICAL BACKGROUND

This study aims to minimize active power losses and average three-phase fault currents separately and simultaneously through reconfiguration under appropriate bus voltage profiles. In this chapter, the mathematical expressions of the optimization process have been shared.

2.1. Reconfiguration

During the reconfiguration scenarios, the radial structure of the test network is maintained in the obtained line topologies. The process of radiality check is explained below [12,26]. Eq. (1) and Eq. (2) represents the number of switches that need to be opened and closed for radial networks.

$$N_{switches}^{opened} = N_{Line} - N_{Bus} + N_{Source} \tag{1}$$

$$N_{switches}^{closed} = N_{Bus} - 1 \tag{2}$$

Additionally, the following criteria must be ensured for radial operation of the test network.

- The loads must be fed from a single source.
- The distribution system must not have a closed loop.
- All nodes must be inside the subgraph

Bus incidence matrix is used to check radiality of the obtained topologies. It is an $N_{Bus}xN_{Line}$ matrix and its elements are determined as follows:

$$\hat{A} = \begin{cases} a_{ij} = \;\;\,0 & \text{if line i is not connected to bus j} \\ a_{ij} = -1 & \text{if line i is oriented towards bus j} \\ a_{ij} = \;\;\,1 & \text{if line i is oriented away bus j} \end{cases} \tag{3}$$

After building bus incidence matrix, the radiality is determined as follows:

$$\det(\hat{A}) = \begin{cases} -1 \text{ or } 1 & \text{Radial} \\ \;\;\;0 & \text{Not Radial} \end{cases} \tag{4}$$

2.2. Power Loss Calculations

One of the main purposes of this study is to minimize active power losses through reconfiguration. The active power loss of a line in the power system is calculated as follows [12]:

$$P_{j,k}^{l} = r_{j,k}.\left|I_{j,k}\right|^{2} \tag{5}$$

In addition, Eq. (6) provides the total power loss in the distribution system, considering the contributions of all branches and incorporating both active and reactive power terms.

It includes a summation over all branches and introduces a switching variable to account for the dynamic structure of the system [27].

$$P^{l}_{Total} = \left(\sum_{i,k=1,}^{N_l} r_{(j,k)} \cdot \left(\frac{{P_k}^2 + {Q_k}^2}{{V_k}^2} \right) . Sw_{(j,k)} \right) \tag{6}$$

2.3. Fault Current Calculations

In this study, the faults occurring in buses are considered as three-phase faults, which are the most dangerous fault type for power systems, and the calculations have been made accordingly. The fault current magnitude at bus n can be found with Eq. (7).

$$I^{f}_{n} = \frac{U_0}{Z_{nn}} \tag{7}$$

During the fault calculations, all pre-fault voltages of the buses are accepted as 1 p.u [28]. The bus admittance matrix is obtained for the different topologies of the test system. Based on this, the column of the impedance matrix that contains the self-impedance (Z_{nn}) for the bus where the fault current is to be calculated can be derived employing Eq. (8) [28].

$$\begin{bmatrix} y_{11} & \cdots & y_{1n} & \cdots & y_{1N} \\ \vdots & \ddots & \vdots & \ddots & \vdots \\ y_{n1} & \cdots & y_{nn} & \cdots & y_{nN} \\ \vdots & \ddots & \vdots & \ddots & \vdots \\ y_{N1} & \cdots & y_{Nn} & \cdots & y_{NN} \end{bmatrix} \begin{bmatrix} z_{1n} \\ \vdots \\ z_{nn} \\ \vdots \\ z_{Nn} \end{bmatrix} = \begin{bmatrix} 0 \\ \vdots \\ 1 \\ \vdots \\ 0 \end{bmatrix} \tag{8}$$

Finally, the AFC of the test system is calculated as below.

$$I_{AFC} = \frac{\sum_{n=1}^{N_{Bus}} (I^{f}_{n})}{N_{Bus}} \tag{9}$$

2.4. Problem Formulation

This study addresses the minimization of average fault currents and total active power losses through single-objective and multi-objective optimization approaches. The study was conducted on 4 cases. In Case 1, the base case of the test system is examined. In Case 2 and Case 3, total active power losses and AFC were minimized through a single-objective optimization studies by using the objective functions in Eq. (10) and Eq. (11), respectively.

$$OF_1 = \min_{x} \left(P^{l}_{Total} \right) \tag{10}$$

$$OF_2 = \min_{x} (I_{AFC}) \tag{11}$$

In Case 4, a multi-objective optimization approach has been applied to investigate the test system in terms of AFC and active power losses according to the objective function given below:

$$OF_3 = \min_{x} (OF_1, OF_2) \tag{12}$$

2.5. Constraints

During the optimization study, the following constraints were considered to ensure stable and safe operation of the test network. Eq. (13) and Eq. (14) represents the voltage limits of the load and source buses, respectively [26,29,30].

$$0.9. V^{i}_{Bus.load} \leq V^{i}_{Bus.load} \leq 1.1. V^{i}_{Bus.load} \tag{13}$$

$$0.95. V^{i}_{Bus.source} \leq V^{i}_{Bus.source} \leq 1.05. V^{i}_{Bus.source} \tag{14}$$

Accordingly, the allowable voltage fluctuations for load and source buses are defined as ±10% and ±5%, respectively. In addition, the constraint ensuring that the transmission capacities of the lines are not exceeded is as follows:

$$I^{i}_{Line} \leq I^{i}_{Line.max.} \tag{15}$$

3. WALRUS OPTIMIZER

In this article, the recently developed Walrus Optimizer has been used to minimize fault currents and power losses [31]. The optimization process in WO begins by using a collection of randomly generated candidate solutions.

$$X = L_{bound} + \mathrm{rand}(U_{bound} - L_{bound}) \tag{16}$$

Walruses act as agents in executing the optimization process, with their positions undergoing continuous updates throughout iterations.

$$X = \begin{bmatrix} X_{1,1}X_{1,2} \dots X_{1,d} \\ X_{2,1}X_{2,2} \dots X_{2,d} \\ \vdots\vdots\vdots \\ X_{n,1}X_{n,2} \dots X_{n,d} \end{bmatrix}_{nxd} \tag{17}$$

$$X = \begin{bmatrix} (f_{1,1}f_{1,2} \dots f_{1,d}) \\ (f_{2,1}f_{2,2} \dots f_{2,d}) \\ \vdots\vdots\vdots \\ (f_{n,1}f_{n,2} \dots f_{n,d}) \end{bmatrix}_{nxd} \tag{18}$$

The walrus population is segmented into adults and immatures, with adults making up 90% and immatures 10% of the total population. The ratio of males to females within the adult walrus population is equal, standing at 1:1. Walruses exhibit high vigilance during foraging and roosting, with 1 to 2 walruses acting as guards that patrol the area. They promptly emit danger signals upon detecting unexpected situations according to the expression below:

$$\text{Danger}_{\text{signal}} = \left(2 - \frac{2.t}{T}\right)(2.\text{rand}(.) - 1) \tag{19}$$

Safety signal is expressed in Eq. (20):

$$\text{Safety}_{\text{signal}} = \text{rand}(.) \tag{20}$$

When risk factors reach a critical level, walrus herds will move to regions more favorable for their survival. During this migration period, the location of the walrus is updated using the following formula:

$$X_{i,j}^{t+1} = X_{i,j}^{t} + (X_m^t - X_n^t).\beta.r_3^2$$
$$\beta = 1 - \frac{1}{1 - e^{\left(-\frac{t-\frac{T}{2}}{T}*10\right)}} \tag{21}$$

Here, $X_{i,j}^{t+1}$ represents the next location for the i^{th} walrus on the j^{th} dimension, $X_{i,j}^{t}$ is the represent the present position of the i^{th} walrus in the j^{th} dimension, Migration step $\left((X_m^t - X_n^t).\beta.r_3^2\right)$ denotes the step size of walrus movement, two vigilantes are randomly chosen from the population, and their locations are represented by X_m^t and X_n^t, β is the migration step control factor that varies smoothly with iteration, and r_3 is a random number between 0 and 1.

The influence of the male walrus $\left(M_{i,j}^t\right)$ and the lead walrus (X_{best}^t) on female walrus changes over iterations, with the female walrus becoming less affected by the mate and more influenced by the leader as the iteration process proceeds.

$$F_{i,j}^{t+1} = F_{i,j}^{t} + \alpha.\left(M_{i,j}^t - F_{i,j}^t\right) + (1-\alpha).\left(X_{best}^t - F_{i,j}^t\right) \tag{22}$$

The next location for the i^{th} female walrus on the j^{th} dimension, denoted as $F_{i,j}^{t+1}$, is determined by considering the positions of the i^{th} male walrus $\left(M_{i,j}^t\right)$ and the current position of the female walrus $\left(F_{i,j}^t\right)$ on that dimension at time t. İmmature walruses situated at the population's edges face threats from killer whales and polar bears, necessitating adjustments to their current positions to evade predation.

$$J_{i,j}^{t+1} = \left(O - J_{i,j}^t\right).P \tag{23}$$

Here, the next position for the i^{th} immature walrus on the j^{th}dimension, denoted as $\left(J_{i,j}^{t+1}\right)$, is determined by considering the current position of the immature walrus $\left(J_{i,j}^t\right)$, the distress coefficient P (a random number between 0 and 1), and the reference safety position O.

$$O = X_{best}^t + J_{i,j}^t.LF \tag{24}$$

Additionally, the position is influenced by LF, a vector of random numbers following a Lévy distribution that represents Lévy movement.

$$\text{Levy}_{\text{flight}}(\alpha) = 0.05.\frac{x}{|y|^{\frac{1}{\alpha}}} \tag{25}$$

where x is N (0, σ_x^2) and y is N (0, σ_y^2). σ_x & σ_y shows the standard deviations and given in Eq. (26).

$$\sigma_x = \left[\frac{\Gamma(1+\alpha)\sin\left(\frac{\pi.\alpha}{2}\right)}{\Gamma\left(\frac{1+\alpha}{2}\right)\alpha^{\frac{\alpha-1}{2}}}\right]^{\frac{1}{\alpha}}, \quad \sigma_y = 1, \quad \alpha = 1.5 \text{ and } \Gamma(q) = \int_0^\infty t^{q-1}.e^{-t}dt \tag{26}$$

where q takes values for all real numbers except negative integers ($q > 0$ and $q \in R$). The graphical representation of the Γ function is typically in the form of a curve and corresponds to factorial values for positive integers.
During underwater foraging, walruses face threats from natural predators and respond by fleeing when they receive danger signals from other walruses. This behavior typically occurs in the later stages of the iteration process in the WO model, and introducing some level of disturbance to the population aids walruses in exploring their environment globally.

$$X_{i,j}^{t+1} = X_{i,j}^{t}.R - \left|X_{best}^{t} - X_{i,j}^{t}\right|.r_4^2 \quad (27)$$

The distance between the best walrus and the current walrus is represented by $\left|X_{best}^{t} - X_{i,j}^{t}\right|$, where r_4 is a randomly generated number within the range of 0 to 1.
Walruses engage in cooperative foraging and movement, using the positions of other walruses in their group. By sharing location details, they enhance the herd's chances of discovering sea areas with more plentiful food sources.

$$\begin{aligned} X_{i,j}^{t+1} &= \frac{(X_1 + X_2)}{2} \\ X_1 &= X_{best}^{t} - \alpha_1.b_1.\left|X_{best}^{t} - X_{i,j}^{t}\right| \\ X_2 &= X_{sec}^{t} - \alpha_2.b_2.\left|X_{sec}^{t} - X_{i,j}^{t}\right| \\ \alpha &= \beta.rand(.) - \beta \\ b &= \tan(\theta) \end{aligned} \quad (28)$$

The gathering behavior of walruses is influenced by two weights, X_1 and X_2. X_{sec}^{t} represents the position of the second walrus in the current iteration, and $\left|X_{sec}^{t} - X_{i,j}^{t}\right|$ indicates the distance between the current walrus and the second walrus. The gathering coefficients α and b play a role, along with a randomly generated number rand(.) within the range of 0 to 1. θ, which represents angles, varies between 0 and π.

4. CASE STUDY

Network reconfiguration allows for enhancements in power systems across various operating parameters. The investigation of the test system with different reconfiguration scenarios was carried out through 4 case studies as shown in table below:

Table 1. Case studies.

	Case 1	Case 2	Case 3	Case 4
Scenarios	Initial Case	Minimizing P_{Total}^{l}	Minimizing I_{AFC}	Minimizing P_{Total}^{l} & AFC
Objective Function	-	$OF_1 = \min_x(P_{Total}^{l})$	$OF_2 = \min_x(I_{AFC})$	$OF_3 = \min_x(OF_1, OF_2)$

4.1. Test System

The case studies within the scope of the study were conducted on the 33-bus test system shared in Figure 1 [23]. It is a widely used benchmark system in the power systems community, providing a standard platform for testing and validating new methodologies [17,20,23]. The system operates at 12.66 kV and it has a single generation unit, 33 buses and 37 switches, including 5 tie switches and 32 sectionalizing switches. The system contains 50751 different radial configuration possibilities. In the base case, the opened switches are S33-S34-S35-S36-S37. During the fault calculations, sub-transient reactance of the generator is accepted as 0.2 p.u.

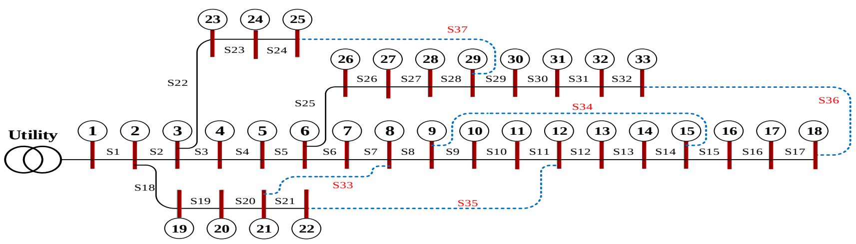

Figure 1. 33-Bus test system [23].

4.2. Results and Discussion

In this section, the results of single-objective and multi-objective optimization studies are shared and evaluated comparatively.

4.2.1. Case 1

Case 1 investigates the employed test system through its base topology, with the open switches S33, S34, S35, S36, and S37. Accordingly, the operational specifications of the test system for Case 1 are as follows:

- Total active and reactive powers in the system are 3.72 MW and 2.3 MVAR, respectively.
- The total power loss in the distribution network is 202.6771 kW and 135.14 kVAr.
- The minimum voltage magnitude in the system is 0.9131 p.u at bus 18.
- The maximum 3-phase fault current magnitude is 5 p.u at bus 1 and the average three-phase fault current for all buses is 2.60 p.u

4.2.2. Case 2 & Case 3

Single-objective optimization studies are carried out in Case 2 and Case 3, focusing on power losses and AFC, respectively. The results for single-objective optimization studies are shared in Table 2, along with the Case 1. Accordingly, in Case 2 focusing on power losses, the active and reactive losses have been reduced to 139.551 kW and j102.297 kVAr, respectively. In the case of this network topology, AFC of the buses has decreased to 2.537 p.u.
In Case 3 focusing on AFC of the buses, AFC value of the network has been reduced to 2.130 p.u. Nevertheless, the active and reactive power losses have increased to 233.040 kW and j189.236 kVAr, respectively.

Table 2. Network operational parameters according to the cases.

	Open Switches (Tie-Switches)	Active Loss **(kW)**	Reactive Loss **(kVAr)**	AFC **(p.u.)**	Min. Voltage **(p.u.)**
Case 1	33-34-35-36-37	202.677	j135.140	2.600	0.913-Bus 18
Case 2	7-9-14-32-37	139.551(-31.146%) *	j102.297(-24.302%) *	2.537(-2.423%) *	0.937-Bus 32
Case 3	3-7-10-21-31	233.040(+14.980%) *	j189.236(+40.029%) *	2.130(-18.076%) *	0.900-Bus 32

***Percentage values were given according to Case 1.**

The comparison of the fault currents for each case is shown in Figure 2 (a). Accordingly, a significant decrease has been achieved in the fault currents of the buses numbered 4-7, 11-14, 22, 26-28 and 32.
Nevertheless, there is a noticeable increase in fault currents only in busbars 29-31. These increases will not cause reliability issues if it remains below the capacity of the circuit breakers, otherwise it can be prevented by using fault current limiters.
On the other hand, in all scenarios, the bus voltages have not fallen below the specified minimum value. Additionally, the best voltage profile was achieved in Case 2. The voltage profile for the test network is shown in Figure 2 (b).

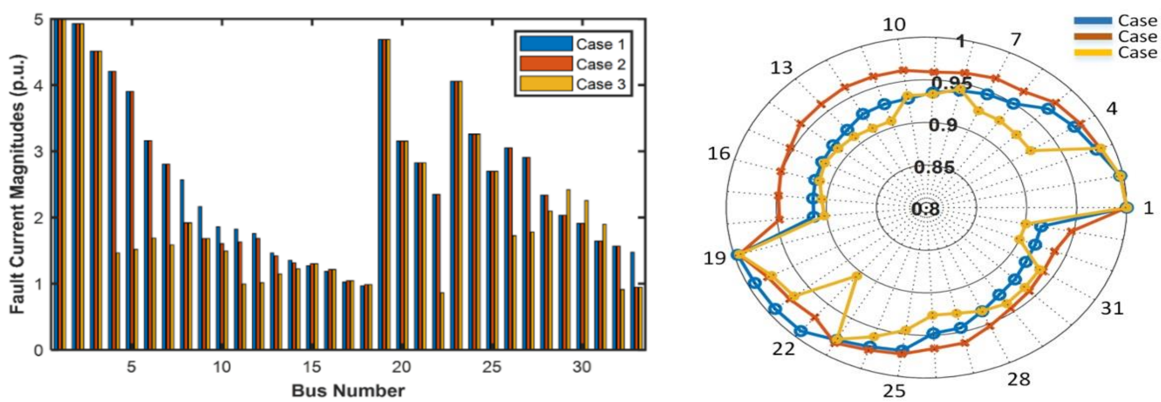

(a) (b)

Figure 2. Results according to the cases (a) bus fault currents (b) bus voltages.

4.2.3. Case 4

As can be seen in Case 2 and Case 3, various parameters are taken into consideration in the operation of the power system and feeder reconfiguration seriously affects these parameters. In this section, a multi - objective optimization study considering AFC and power losses has been carried out. As the result of the study, different network topologies have been obtained. Accordingly, AFC and power loss results for obtained topologies are shared in Figure 3.
Optimal Pareto solutions are shown in red circles as non-dominated solutions. A solution is defined as dominated if it is worse than at least one other solution in all considered objective functions. On the other hand, a solution is considered non-dominated or Pareto optimal solution if there is no other solution that improves one objective without degrading another. Non-dominated solutions have the AFC value between 2.130 p.u and 2.537 p.u, representing a change of -18.076% to -2.423% compared to original case. Additionally, active power loss changes between 139.551 kW and 233.04 kW, corresponding to a change of -31.146% to 14.980% compared to original case. As can be seen that, numerous network topologies exist which have lower AFC value and reduced power

losses compared to the base case. All dominated and non-dominated solutions are listed in Table 3. Additionally, it is observed that the average fault current and power losses change inversely. Depending on the current needs of the power system, the operational topology can be decided by prioritizing either reliability or economy.

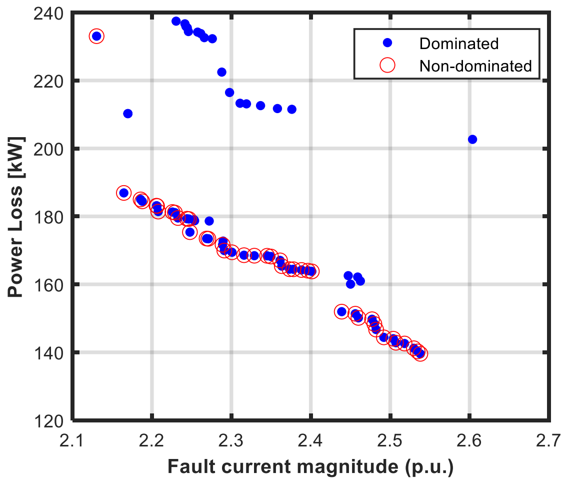

Figure 3. $I_{Fault}^{average}$ vs active power losses for different optimal network topologies.

Table 3. Dominated and non-dominated results.

Open Switches	$I_{Fault}^{average}$ (p.u.)	Active loss (kW)	Reactive Loss (kVAr)	Min. Bus Voltage (p.u.)
11-12-18-25-36	2.3761	211.5065	146.6899	0.9278
11-12-18-25-32	2.3580	211.7351	147.2179	0.9248
8-14-17-18-25	2.2459	234.3931	169.2775	0.9064
3-9-15-21-28	2.1697	210.2430	170.8469	0.9126
11-14-18-25-32	2.3367	212.5978	148.7414	0.9236
9-12-18-25-32	2.3190	213.1118	148.9607	0.9258
9-13-18-25-31	2.2879	222.4600	158.4661	0.9079
9-13-18-25-32	2.3109	213.2908	149.3724	0.9277
9-14-18-25-32	2.2977	216.4597	152.8585	0.9183
7-11-25-31-34	2.4500	160.0613	128.9963	0.9155
3-8-11-17-28	2.2064	183.0589	148.2700	0.9316
4-8-11-17-28	2.2896	172.7313	137.4788	0.9346
6-9-14-25-32	2.4624	160.9720	125.1944	0.9376
6-11-25-32-34	2.4471	162.5563	127.1410	0.9357
8-11-15-18-25	2.2445	235.4989	169.1125	0.9095
3-8-9-28-36	2.2289	181.1149	148.8970	0.9279
8-10-15-18-25	2.2575	234.2205	167.9628	0.9125
6-11-32-34-37	2.4919	144.4019	111.0024	0.9357
8-10-17-18-25	2.2304	237.4514	172.3620	0.9011
8-9-17-18-25	2.2428	235.9099	170.9528	0.9039
3-10-26-34-36	2.2721	178.6311	143.9372	0.9349
8-14-15-18-25	2.2760	232.2825	166.0951	0.9154
8-14-16-18-25	2.2659	232.6021	167.0269	0.9137
8-13-17-18-25	2.2415	236.6772	170.9970	0.9016
3-11-25-32-34	2.2465	179.2272	144.9568	0.9302
8-9-16-18-25	2.2614	233.8085	168.3061	0.9101
6-8-11-36-37	2.4560	151.3593	115.9789	0.934
3-8-14-28-32	2.2079	181.4116	150.3277	0.9215
5-10-28-34-36	2.4013	163.8116	130.7143	0.9368
3-10-28-32-34	2.1697	210.2430	170.8469	0.9126
4-11-27-34-36	2.3450	168.4078	134.3007	0.9381
4-8-11-28-36	2.2710	173.4174	140.5817	0.9278
4-10-27-34-36	2.3498	168.1951	134.2584	0.9366
3-11-26-32-34	2.2441	179.3020	146.2572	0.9289
4-8-11-28-32	2.2478	175.3626	144.2627	0.9205
3-9-28-32-34	2.2258	181.2891	150.7076	0.9234
4-10-28-32-34	2.1697	210.2430	170.8469	0.9126
4-10-28-34-36	2.3289	168.4310	135.5913	0.9354
3-8-14-17-28	2.2530	179.0256	144.2372	0.9353
3-8-11-28-36	2.1878	184.4317	151.9827	0.9248

Table 3. Dominated and non-dominated results (continued).

Open Switches	$\mathbf{I_{Fault}^{average}}$ $(\mathbf{p.u.})$	Active loss $(\mathbf{kW})$	Reactive Loss $(\mathbf{kVAr})$	Min. Bus Voltage $(\mathbf{p.u.})$
5-8-14-28-36	2.3883	164.2258	130.9733	0.9339
5-8-14-28-32	2.3635	165.3620	133.7157	0.9259
3-8-11-28-32	2.1646	186.9037	156.1334	0.9174
4-8-9-28-32	2.2889	171.6518	140.8099	0.9234
3-8-14-28-36	2.2327	179.5253	146.9197	0.9296
6-8-9-32-37	2.4800	148.3554	115.3673	0.9297
7-9-14-31-37	2.5180	142.5943	111.1480	0.9239
5-8-9-28-32	2.3613	167.0570	135.9807	0.9248
3-8-9-28-32	2.2057	183.1426	152.6331	0.9204
4-8-10-28-32	2.2688	173.4816	142.5228	0.9219
4-8-14-28-36	2.3159	168.5772	135.5842	0.9326
6-8-10-36-37	2.4771	149.7326	114.4766	0.9356
6-8-10-32-37	2.3964	164.0148	130.7472	0.9382
5-11-28-34-36	2.4599	150.1355	117.0332	0.9282
7-11-14-32-37	2.5297	141.1947	103.5577	0.9378
4-8-14-28-32	2.2911	169.9459	138.5327	0.9245
* **7-9-14-32-37**	2.5379	139.5513	102.2979	0.9378
6-10-14-25-32	2.4590	162.1550	126.1771	0.9371
6-8-14-32-37	2.4822	146.6985	113.1454	0.9308
6-10-14-32-37	2.5039	144.0007	110.0386	0.9372
6-9-14-32-37	2.5072	142.8178	109.0560	0.9388
6-8-11-32-37	2.4389	151.9654	118.7249	0.9267
5-10-28-32-34	2.3781	164.4448	133.1248	0.9293
4-11-28-32-34	2.3008	169.4359	138.1627	0.9294
5-11-28-32-34	2.3732	164.4663	132.9632	0.9308
3-8-10-28-32	2.1857	184.9971	154.3695	0.9189
7-10-14-32-37	2.5345	140.2695	102.8314	0.9378
3-8-14-27-36	2.2537	178.7208	145.0745	0.9308
** **3-7-10-21-31**	2.1303	233.0399	189.2367	0.9001
33-34-35-36-37	2.6036	202.6619	135.1309	0.9131

***Min active power loss switch-configuration ** Min average fault current switch-configuration**

5. CONCLUSION

In this study, Walrus Optimizer, a recently developed algorithm, is used for optimizing the reconfiguration of distribution networks to minimize fault currents and active power losses. The effectiveness of this approach is demonstrated through a series of case studies conducted on the IEEE 33-bus test system.

The results of the single-objective optimization scenarios (Cases 2 and 3) reveal significant improvements in both power loss reduction and fault current minimization. Specifically, the optimal configuration achieved in Case 2 reduce active and reactive power losses to 139.551 kW and 102.297 kVAr, respectively, while maintaining acceptable fault current levels. Conversely, in Case 3, the AFC is minimized to 2.130 $\mathrm{p.u}$, though this is accompanied by an increase in power losses to 233.04 kW and 189.236 kVAr.

The multi-objective optimization study (Case 4) provides a comprehensive understanding of the trade-offs between power losses and fault currents. Notably, the non-dominated solutions achieve a range of AFCs between 2.130 $\mathrm{p.u}$ and 2.537 $\mathrm{p.u}$, with corresponding active power losses varying from 139.551 kW to 233.04 kW. Considering the base scenario's active power loss of 202.67 kW and the AFC value of 2.60 $\mathrm{p.u}$, the multi-objective optimization study reveals many optimal reconfigurations that achieve superior power loss and AFC values. Referring to the results, the Pareto optimal solutions demonstrate that feeder reconfiguration can address multiple operational criteria, balancing reliability and economic efficiency according to the system's requirements.

The results provide new insights into managing fault currents and power losses, as well as understanding the trade-offs between these objectives while maintaining suitable bus voltage profiles through a novel algorithm for optimizing power systems.

Future research will aim to integrate the allocation of Distributed Generation (DG) and Fault Current Limiter (FCL) systems alongside reconfiguration strategies to further optimize power losses and fault currents, thereby ensuring greater reliability and efficiency in power distribution networks.

Author Contributions

All stages of the study were done by the authors.

Statement of Conflict of Interest

Authors have declared no conflict of interest.

REFERENCES

[1] Y. Varetsky and M. Gajdzica, “Study of Short Circuit and Inrush Current Impact on the Current-Limiting Reactor Operation in an Industrial Grid,” Energies (Basel), vol. 16, no. 2, 2023.

[2] R. Razzaghi and K. Niayesh, “Current limiting reactor allocation in distribution networks in presence of distributed generation,” in 2011 10th International Conference on Environment and Electrical Engineering, IEEE, pp. 1–4, 2011.

[3] A.O. Surya, L. Gumilar, M.A. Habibi, A. Kusumawardana, A.N. Afandi, and Aripriharta, “Increase in High Impedance Value of Transformer to Reduce Short Circuit Fault Currents in High Voltage Networks,” in Proceedings - 11th Electrical Power, Electronics, Communications, Control, and Informatics Seminar, EECCIS 2022, Institute of Electrical and Electronics Engineers Inc., pp. 51–55, 2022.

[4] Y. Li, B. Liu, Y. Zhu, J. Hou, R. Liu, and L. Guo, “High-impedance transformer parameter determination method for limiting short-circuit current of power system,” in 22nd International Conference on Electrical Machines and Systems (ICEMS), pp. 1-5, Harbin, China, 2019.

[5] O. Arikan and B. Kucukaydin, “A new approach to limit fault current with series–parallel resonance strategy,” Electrical Engineering, vol. 102, no. 3, pp. 1287-1296, 2020.

[6] F. Akin, O. Arikan, and B. Kucukaydin, “Multi-physics modelling and performance analysis of an air-core reactor in the framework of solid-state fault current limiters,” Electric Power Systems Research, vol. 231, 2024.

[7] S. Namchoat and N. Hoonchareon, “Optimal bus splitting for short-circuit current limitation in metropolitan area,” in 10th International Conference on Electrical Engineering/Electronics, Computer, Telecommunications and Information Technology, pp. 1-5, Krabi, Thailand, 2013.

[8] P. Kanlaya and N. Hoonchareon, “Combined bus splitting and line bypassing for short-circuit currents limitation,” in 10th International Conference on Electrical Engineering/Electronics, Computer, Telecommunications and Information Technology, pp. 1-6, Krabi, Thailand, 2013.

[9] P.K. Sanodiya, M.V. Rao, C. Ghangrekar, V. Pandey, S. Pushpa, and K. Muralikrishna, “Limiting short circuit levels through network reconfiguration: An experience in India,” in 21st National Power Systems Conference, NPSC, pp. 1-5, Kharagpur, India, 2020.

[10] Z. Yang, H. Zhong, Q. Xia, and C. Kang, “Optimal transmission switching with short-circuit current limitation constraints,” IEEE Transactions on Power Systems, vol. 31, no. 2, pp. 1278-1288, 2016.

[11] M. Rahimipour Behbahani and A. Jalilian, “Reconfiguration of distribution network for improving power quality indexes with flexible lexicography method,” Electric Power Systems Research, vol. 230, 2024.

[12] M. Cikan and B. Kekezoglu, “Comparison of metaheuristic optimization techniques including Equilibrium optimizer algorithm in power distribution network reconfiguration,” Alexandria Engineering Journal, vol. 61, no. 2, pp. 991-1031, 2022.

[13] V.J. Shetty and S.G. Ankaliki, “Electrical Distribution System Power Loss Reduction and Voltage Profile Enhancement by Network Reconfiguration Using PSO,” in 2019 Fifth International Conference on Electrical Energy Systems (ICEES), IEEE, pp. 1–4, 2019.

[14] A. Amin, A.Y. Abdelaziz, M.A. Attia, and M. Zakaria Kamh, “Optimal reconfiguration for Extra high voltage transmission networks using an enhanced Brute-Force algorithm,” Ain Shams Engineering Journal, vol. 14, no. 12, 2023.

[15] D. Topolanek et al., “Optimization method for short circuit current reduction in extensive meshed LV network,” International Journal of Electrical Power & Energy Systems, vol. 152, p. 109203, Oct. 2023.

[16] A. Parizad, H.R. Baghaee, A. Yazdani, and G.B. Gharehpetian, “Optimal distribution systems reconfiguration for short circuit level reduction using PSO algorithm,” in 2018 IEEE Power and Energy Conference at Illinois (PECI), IEEE, pp. 1–6, 2018.

[17] S.A. Ahmadi, V. Vahidinasab, M.S. Ghazizadeh, and D. Giaouris, “A stochastic framework for secure reconfiguration of active distribution networks,” IET Generation, Transmission and Distribution, vol. 16, no. 3, pp. 580–590, 2022.

[18] X. Zhang, Y. Liu, J. Zhao, J. Liu, M. Korkali, and X. Chen, “Short-circuit current constrained unit commitment and transmission switching model for improving renewable integration: An MILP formulation,” IET Generation, Transmission and Distribution, vol. 16, no. 9, pp. 1743–1755, 2022.

[19] S. Kong, H.C. Jo, Y.M. Wi, and S.K. Joo, “Optimization-Based Reconfiguration Method for Power System Incorporating Superconducting Fault Current Limiter Failure,” IEEE Transactions on Applied Superconductivity, vol. 26, no. 4, 2016.

[20] W. Guan, Y. Tan, H. Zhang, and J. Song, “Distribution system feeder reconfiguration considering different model of DG sources,” International Journal of Electrical Power and Energy Systems, vol. 68, pp. 210–221, 2015.

[21] D.F. Teshome and K.L. Lian, “Comprehensive mixed-integer linear programming model for distribution system reconfiguration considering DGs,” IET Generation, Transmission and Distribution, vol. 12, no. 20, pp. 4515–4523, 2018.

[22] M. Abd El-salam, E. Beshr, and M. Eteiba, “A New Hybrid Technique for Minimizing Power Losses in a Distribution System by Optimal Sizing and Siting of Distributed Generators with Network Reconfiguration,” Energies (Basel), vol. 11, no. 12, p. 3351, 2018.

[23] S. Kamel, M. Khasanov, F. Jurado, A. Kurbanov, H. M. Zawbaa, and M.A. Alathbah, “Simultaneously Distributed Generation Allocation and Network Reconfiguration in Distribution Network Considering Different Loading Levels,” IEEE Access, vol. 11, pp. 105916–105934, 2023.

[24] M. Mahdavi, K.E.K. Schmitt, and F. Jurado, “Robust Distribution Network Reconfiguration in the Presence of Distributed Generation under Uncertainty in Demand and Load Variations,” IEEE Transactions on Power Delivery, vol. 38, no. 5, pp. 3480–3495, 2023.

[25] L.H. Macedo, J.M. Home-Ortiz, R. Vargas, J.R.S. Mantovani, R. Romero, and J.P.S. Catalão, “Short-circuit constrained distribution network reconfiguration considering closed-loop operation,” Sustainable Energy, Grids and Networks, vol. 32, 2022.

[26] N. Nacar Cikan and M. Cikan, “Reconfiguration of 123-bus unbalanced power distribution network analysis by considering minimization of current & voltage unbalanced indexes and power loss,” International Journal of Electrical Power and Energy Systems, vol. 157, 2024.

[27] M.E. Baran and F.F. Wu, “Network reconfiguration in distribution systems for loss reduction and load balancing,” IEEE Transactions on Power Delivery, vol. 4, no. 2, pp. 1401–1407, 1989.

[28] H. Hua et al., “Optimal Allocation and Sizing of Fault Current Limiters Considering Transmission Switching With an Explicit Short Circuit Current Formulation,” IEEE Transactions on Power Systems, vol. 38, no. 2, pp. 1322–1335, 2023.

[29] E.F. Fuchs, M.A.S. Masoum, “Introduction to power quality,” in Power Quality in Power Systems, Electrical Machines, And Power-Electronic Drives, 3rd ed. London, United Kingdom: Academic Press, 2023.

[30] V.M. Hrishikesan et. al.,“Capacity Enhancement of a Radial Distribution Grid Using Smart Transformer,” IEEE Access, vol. 8, pp. 72411–72423, 2020.

[31] M. Han, Z. Du, K. F. Yuen, H. Zhu, Y. Li, and Q. Yuan, “Walrus optimizer: A novel nature-inspired metaheuristic algorithm,” Expert Syst Appl, vol. 239, 2024.